Modeling of open quantum devices within the closed-system paradigm

Remo Proietti Zaccaria,* Emanuele Ciancio,† Rita C. Iotti,‡ and Fausto Rossi§
Istituto Nazionale per la Fisica della Materia (INFM) and Dipartimento di Fisica, Politecnico di Torino, Corso Duca degli Abruzzi 24, 10129 Torino, Italy
(Received 27 January 2004; published 10 November 2004)

We present an alternative simulation strategy for the study of nonequilibrium carrier dynamics in quantum devices with open boundaries. We propose to replace the usual modeling of open quantum systems based on phenomenological injection/loss rates with a kinetic description of the system-reservoir thermalization process. In this simulation scheme the partial carrier thermalization induced by the device spatial boundaries is treated within the standard Boltzmann-transport approach via an effective scattering mechanism between the highly nonthermal device electrons and the thermal carrier distribution of the reservoir. Applications to state-of-the-art semiconductor nanostructures are discussed. Finally, the proposed approach is extended to the quantum-transport regime; to this end, we introduce an effective Liouville superoperator, able to describe the effect of the device spatial boundaries on the time evolution of the single-particle density matrix.

DOI: 10.1103/PhysRevB.70.195311 PACS number(s): 73.40.−c, 85.30.−z, 72.10.Bg

I. INTRODUCTION

The never-ending scaling-down of typical space and time scales in quantum optoelectronic devices leads to physical conditions where the traditional Boltzmann transport theory[1] can no longer be employed, thus demanding for reliable quantum-transport approaches.[2] In spite of the quantum-mechanical nature of carrier dynamics in the core region of typical nanostructured devices (like, e.g., semiconductor superlattices and double-barrier structures), however, the overall behavior of such quantum systems often results from a nontrivial interplay between phase coherence and dissipation,[3] the latter being primarily due to the presence of spatial boundaries.[4] A rigorous theoretical modeling of such new-generation nanoscale devices should therefore simultaneously account for both coherent and incoherent—i.e., phase-breaking—processes on equal footing. In this context, a generalization to open systems (that is, systems with open boundaries coupling them to external charge reservoirs), of the well known semiconductor Bloch equations (SBEs)[5] has been recently proposed.[6,7] Such fully microscopic treatments, which are essential for the basic understanding of the quantum phenomena involved, are often extremely computer-time consuming. Therefore they cannot be employed in standard optoelectronic-device modeling and optimization where, in contrast, partially phenomenological (and computationally affordable) models[8,9] are usually considered. Among such simulation strategies it is worth mentioning the approach proposed by Fischetti and co-workers.[10] This is grounded on a Master Equation description derived from a rigorous density-matrix formulation of the problem, and can be regarded as the diagonal (i.e., semiclassical) limit of the theoretical scheme proposed in Ref. 6. Within such partially phenomenological treatments, however, the coupling of the quantum device with external reservoirs is typically described in terms of extremely simplified injection/loss models.[8–10]

In this paper we present an alternative simulation strategy for the study of nonequilibrium carrier dynamics in quantum devices with open boundaries. In particular, we propose to replace the usual modeling of open quantum systems, based on phenomenological injection/loss rates, with a kinetic description of the system-reservoir thermalization process. Within this simulation scheme the partial carrier thermalization induced by the device spatial boundaries can be treated via a conventional Monte Carlo (MC) sampling of the Boltzmann equation: this is done in terms of an effective scattering mechanism between the highly nonthermal device electrons and the thermal carrier distribution of the reservoir. As we shall see, in this approach the total number of simulated electrons is conserved (closed picture); this is a distinguished advantage of the proposed strategy, contrary to hybrid—direct numerical-integration plus MC-sampling—methods, where the total number of particles is not constant (open picture).

As a second step, we shall extend the proposed particle-conserving kinetic approach to the quantum-transport regime. More specifically, similar to the semiclassical case, we shall introduce a Liouville superoperator able to properly describe carrier thermalization/dephasing due to the coupling with the external reservoirs.

The paper is organized as follows. In Sec. II we shall recall the standard approach and introduce the simulation strategy; to show the power and flexibility of the proposed theoretical scheme, the latter is applied to the study of hot-carrier transport phenomena in bulk systems as well as in semiconductor nanostructures, like resonant-tunneling diodes and quantum-dot devices. Section III is devoted to the generalization of the proposed simulation strategy to the quantum-transport regime. Finally, in Sec. IV we shall summarize and draw some conclusions.

II. PROPOSED SIMULATION STRATEGY

We start by recalling the main features of the typical approach employed in the simulation of state-of-the-art semiconductor-based quantum devices. Let f_α be the carrier distribution over the electronic states α of the device.[11] The equation governing hot-carrier transport/relaxation phenom-

ena in open systems may be schematically written as[12]

$$\frac{d}{dt}f_\alpha = \left.\frac{d}{dt}f_\alpha\right|_{\text{scat}} + \left.\frac{d}{dt}f_\alpha\right|_{\text{res}}. \tag{1}$$

The first term describes scattering dynamics within the device active region and is usually treated at a kinetic level via a Boltzmann-like collision operator of the form

$$\left.\frac{d}{dt}f_\alpha\right|_{\text{scat}} = \sum_{\alpha'} (P^s_{\alpha\alpha'}f_{\alpha'} - P^s_{\alpha'\alpha}f_\alpha), \tag{2}$$

here $P^s_{\alpha\alpha'}$ is the total (i.e., summed over all relevant interaction mechanisms) scattering rate from state α' to state α.

The last term in (1) accounts for the open character of the system and describes injection/loss contributions from/to the (at least two) external carrier reservoirs. These processes are usually modeled by a relaxation-time-like term of the form[10]

$$\left.\frac{d}{dt}f_\alpha\right|_{\text{res}} = -\gamma_\alpha(f_\alpha - f^0_\alpha) = G_\alpha - \gamma_\alpha f_\alpha, \tag{3}$$

here γ_α^{-1} may be interpreted as the ballistic transit time for an electron in state α,[13] while f^0_α is the carrier distribution in the external reservoirs. The latter may correspond to the distinct quasiequilibrium distributions in the left and right chemical potentials, or may describe a generic nonequilibrium distribution within the external reservoirs.

In spite of the kinetic nature of the scattering dynamics in (2), the contribution in (3) describes carrier injection and loss processes on a partially phenomenological level; this, in turn, requires hybrid simulation strategies[14] combining a MC sampling of the scattering dynamics with a direct numerical integration of injection/loss terms.

In what follows we propose to replace the conventional relaxation-time term in (3) with a Boltzmann-like operator of the form

$$\left.\frac{d}{dt}f_\alpha\right|_{\text{res}} = \sum_{\alpha'} (P^r_{\alpha\alpha'}f_{\alpha'} - P^r_{\alpha'\alpha}f_\alpha), \tag{4}$$

this contribution has indeed the same structure of the scattering operator in (2); however, the new scattering rates $P^r_{\alpha\alpha'}$ describe electronic transitions within the simulated region induced by the coupling to the external carrier reservoirs. It is worthwhile to stress that, contrary to the conventional injection/loss term in (3), in this case there is no particle exchange between device active region and thermal reservoirs. The total number of simulated particles is therefore conserved.

Let us now discuss the explicit form of the rates $P^r_{\alpha\alpha'}$ entering Eq. (4). In the absence of scattering processes ($P^s_{\alpha\alpha'}=0$), the steady-state solution of the conventional injection/loss model in (3) is $f_\alpha = f^0_\alpha$, i.e., the carrier distribution inside the device coincides with the distribution in the external carrier reservoirs. As a first requirement, we therefore impose the same steady-state solution ($f_\alpha = f^0_\alpha$) to the new collision operator in (4). This, in turn, will impose conditions on the explicit form of the scattering rates $P^r_{\alpha\alpha'}$. More specifically, from the detailed-balance principle[1] we get[15]

$$\frac{P^r_{\alpha\alpha'}}{P^r_{\alpha'\alpha}} = \frac{f^0_\alpha}{f^0_{\alpha'}}. \tag{5}$$

It follows that our transition rates should be of the form

$$P^r_{\alpha\alpha'} = \mathcal{P}_{\alpha\alpha'}f^0_\alpha, \tag{6}$$

where $\mathcal{P}$ can be any positive and symmetric transition matrix ($\mathcal{P}_{\alpha\alpha'} = \mathcal{P}_{\alpha'\alpha} > 0$). What is important in steady-state conditions is the ratio of the scattering rates in (5) and not their absolute values which are, in contrast, crucial in determining the transient nonequilibrium response of the system. Since our aim is to replace the injection/loss term in (3) with the Boltzmann-like term in (4), as second requirement we ask that the relaxation dynamics induced by the new collision term corresponds to the phenomenological relaxation times in (3). This corresponds to imposing that the total out-scattering rate—summed over all possible final states—coincides with the relaxation rates γ_α:

$$\Gamma_\alpha \equiv \sum_{\alpha'} P^r_{\alpha'\alpha} = \gamma_\alpha. \tag{7}$$

By assuming—as simplest form of the symmetric transition matrix in (6)—$\mathcal{P}_{\alpha\alpha'} = p_\alpha p_{\alpha'}$, Eq. (7) reduces to the following system of equations for the unknown quantities p_α:

$$\sum_{\alpha'} p_{\alpha'}f^0_{\alpha'} = \frac{\gamma_\alpha}{p_\alpha}. \tag{8}$$

Since the sum on the left is α-independent, we immediately get: $p_\alpha \propto \gamma_\alpha$. Starting from this result, we finally obtain

$$\mathcal{P}_{\alpha\alpha'} = p_\alpha p_{\alpha'} = \frac{\gamma_\alpha\gamma_{\alpha'}}{\sum_{\alpha''}\gamma_{\alpha''}f^0_{\alpha'}}. \tag{9}$$

The explicit form of the desired system-reservoir scattering rates entering the Boltzmann-like collision term in (4) may be derived by combining Eqs. (6) and (9). As stated earlier, the proposed kinetic formulation in terms of Boltzmann-like collision operators only, is particularly suited for a standard ensemble-MC simulation approach, where one deals with a fixed number of particles. In this respect, contrary to the phenomenological model in Eq. (3), in the present closed-system formulation the total carrier density is not fixed by the external reservoirs and the resulting transport equation is homogeneous.

To test the proposed simulation strategy, we have developed a fully three-dimensional (3D) MC simulator, using as basis states α the product of scattering states along the field/growth direction, and two-dimensional plane waves accounting for the in-plane dynamics. In order to properly describe phonon-induced energy and momentum relaxation within the device active region, carrier-phonon scattering in a fully 3D fashion has been included,[16] in addition to the new scattering-like thermalization mechanism in (4).

We start considering an extremely simple transport problem: a GaAs mesoscopic bulk system of length $l=200$ nm sandwiched between two reservoirs with different chemical

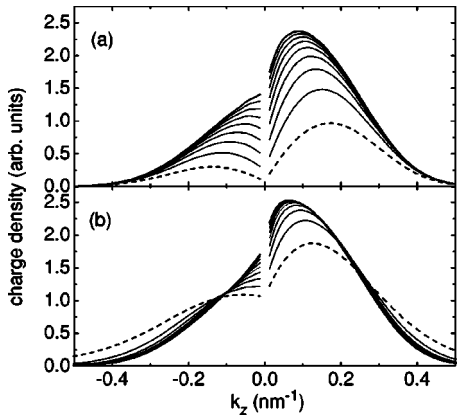

FIG. 1. Room-temperature transport properties of a GaAs mesoscopic bulk system of length $l=200$ nm sandwiched between two reservoirs with different chemical potentials ($\mu_{\text{left}}-\mu_{\text{right}}=50$ meV). Transient dynamics of the carrier distribution in momentum space—from 1 ps (dashed curve) to 9 ps (thick solid curve) at intervals of 1 ps (thin solid curves)—as obtained (a) from the conventional injection/loss model in (3) and (b) from the proposed simulation strategy.

potentials ($\mu_{\text{left}}-\mu_{\text{right}}=50$ meV). We have applied to this problem the simulation strategy previously described [see Eq. (4)] and have compared the results with those of the conventional simulation approach [see Eq. (3)].

Figure 1(a) presents the transient carrier dynamics resulting from the conventional injection/loss model in (3). Here, we show the time evolution of the carrier distribution in momentum space at steps of 1 ps. Since in this model we start at time $t=0$ with an empty-device configuration, the simulated experiment shows a progressive increase of the carrier distribution, which from the very beginning exhibits a strong left-right asymmetry in momentum space due to the chemical-potential misalignment. This scenario manifests the open nature of the conventional approach, which does not allow the direct use of a standard MC procedure. It is worthwhile to stress that the driving force responsible for charge transport is the difference of quasiequilibrium chemical potentials describing the left and right carrier distributions *entering* the device active region and not the difference of carrier concentrations within the two electrical contacts. Indeed, the total (entering plus exiting) carrier density is rigorously homogeneous through the whole structure since we are dealing with a simple bulk model whose single-particle states are plane waves. The situation is different in momentum space, where momentum-relaxation effects are observed due to the fact that we are dealing with a quasiballistic regime (i.e., the ballistic motion of the injected electrons is disturbed by phonon-induced scattering). In the present simulated experiment we have a total carrier concentration (which has been directly evaluated from the thermal distributions f_α^0) of about 7×10^{17} cm^{-3}, while the left and right injected carrier concentrations are, respectively, of about 6.2×10^{17} cm^{-3} and 8×10^{16} cm^{-3}.

Figure 1(b) shows again the transient evolution of the carrier distribution in momentum space, but obtained from the proposed simulation approach. In this case we deal with

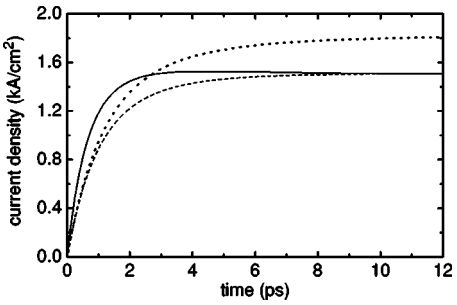

FIG. 2. Charge current density as a function of time corresponding to the two simulated experiments in Figs. 1(a) (dashed curve) and 1(b) (solid curve). The scattering-free or ballistic result (dotted curve) is also reported (see text).

a fixed number of particles which at time $t=0$ are arbitrarily chosen to be equally distributed in the 3D momentum space. Moreover, the total carrier density, which is now a free parameter, has been set equal to the steady-state value in (a). Contrary to the time evolution in (a), here at very short times the device region is already occupied and its charge distribution in momentum space is almost symmetric. Only at later times, due to the effective scattering mechanism in (6), we recover the asymmetric distribution of Fig. 1(a) (see solid curve).

Figure 2 shows the charge current density as a function of time corresponding to the two simulated experiments in Fig. 1(a) (dashed curve) and Fig. 1(b) (solid curve). At time $t=0$ the current is in both cases equal to zero; this is, however, ascribed to different reasons: in Fig. 1(a) at $t=0$ the carrier density is equal to zero while the mean velocity is different from zero; in Fig. 1(b) the mean velocity is equal to zero while the carrier density is different from zero. In spite of a slightly different transient, both curves reach almost the same steady-state value, confirming the validity of the proposed simulation strategy.[17]

The steady-state regime results from a strong interplay between the thermalization induced by the external reservoirs and the phonon-induced momentum relaxation within the device active region. Indeed, in the phonon-free case (dotted curve in Fig. 2) the steady-state current—which is fully ballistic—reaches significantly higher values. The momentum-relaxation dynamics previously mentioned is clearly visible in Fig. 1(a), where the peaks of the injected carrier distribution are progressively shifted to lower wave vectors.

As a second testbed, we have considered a prototypical semiconductor quantum device: a GaAs/AlGaAs resonant-tunneling diode with a barrier height of 0.24 eV and a barrier width and separation of 2.8 and 4.4 nm, respectively. Figure 3 shows the current-voltage characteristics obtained from the proposed MC simulation scheme with (solid curve) and without (dashed curve) carrier-phonon scattering. The results demonstrate that we are able to properly describe the typical resonance scenario. More specifically, as expected, in the presence of phase-breaking processes, like carrier-phonon scattering, the resonance peak is significantly reduced. Also in this more realistic case the proposed simulation strategy comes out to properly describe the key phenomena under investigation.

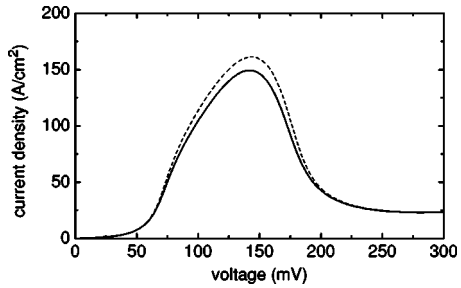

FIG. 3. Room-temperature current-voltage characteristics of a GaAs/AlGaAs resonant-tunneling diode (with barrier height 0.24 eV and barrier width and separation of 2.8 and 4.4 nm, respectively) as obtained from our MC simulation scheme with (solid curve) and without (dashed curve) carrier-phonon scattering.

As a final example, we have considered a typical nonequilibrium situation, an electrically-driven quantum-dot system. To this end, we have adopted an extremely simplified model: an electronic two-level system coupled to the phonon modes of the host materials as well as to two external (injecting and extracting) charge reservoirs (see inset in Fig. 4).

According to the general prescription previously introduced [see Eq. (2)], by denoting with a and b the ground and excited states of our two-level system, the phonon-induced scattering dynamics will be described in terms of two interlevel rates corresponding to phonon absorption and emission

$$P^s_{ba} = W^s N, \quad P^s_{ab} = W^s(N+1), \tag{10}$$

where $N=(e^{\Delta\epsilon/k_BT}-1)^{-1}$ is the Bose occupation number corresponding to the interlevel energy splitting $\Delta\epsilon=\epsilon_b-\epsilon_a$. In the absence of coupling to the external reservoirs, regardless of the value of the carrier-phonon coupling constant W^s, the steady-state solution is the thermal equilibrium one

$$\mathcal{R}^{\rm eq} = \frac{f^{\rm eq}_b}{f^{\rm eq}_a} = \frac{P^s_{ba}}{P^s_{ab}} = \frac{N_B}{N_B+1} = e^{-\Delta\epsilon/k_BT}. \tag{11}$$

In contrast, in the presence of external reservoirs characterized by different values of their chemical potentials, $\mu_{\rm left}$ and $\mu_{\rm right}$ (see inset in Fig. 4), the population ratio $\mathcal{R}$ may differ significantly from the thermal-equilibrium value in (11). More specifically, in the absence of phonon-induced interlevel scattering ($W^s=0$) the population ratio $\mathcal{R}_0$ is fully dictated by the carrier distributions within the reservoirs, and may be greater than one, i.e., a population-inversion regime may be established.

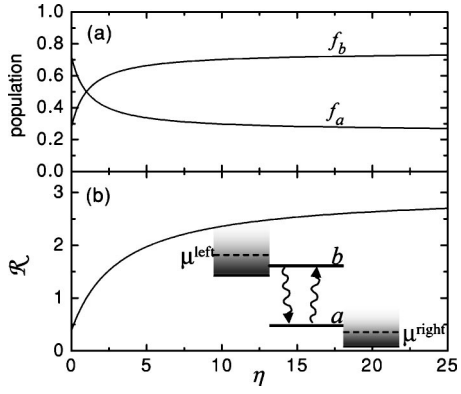

FIG. 4. Electrically driven nonequilibrium carrier distribution in a quantum-dot system: (a) excited- and ground-state populations f_b and f_a and (b) their ratio $\mathcal{R}$ as a function of the coupling-constant ratio η, for an interlevel energy splitting $\Delta\epsilon=25$ meV and for a reservoir-induced population ratio $\mathcal{R}_0=3$ at room temperature (see text). A schematics of the electrically driven two-level system is also reported in the inset.

Following again the proposed simulation strategy, we shall describe the effect of the system-reservoir coupling in terms of the effective Boltzmann collision term in (4). More specifically, for the case of our two-level system we have

$$P^r_{ba} = W^r \frac{\mathcal{R}_0}{\mathcal{R}_0+1}, \quad P^r_{ab} = W^r \frac{1}{\mathcal{R}_0+1}, \tag{12}$$

where W^r denotes a suitable system-reservoir coupling constant. Analogous to Eq. (11), it is easy to see that, in the absence of carrier-phonon scattering, such effective rates provide as steady-state solution the desired population ratio $\mathcal{R}_0$, i.e.,

$$\frac{f^0_b}{f^0_a} = \frac{P^r_{ba}}{P^r_{ab}} = \mathcal{R}_0. \tag{13}$$

In the presence of carrier-phonon scattering as well as coupling to the external reservoirs, the actual value of the population ratio $\mathcal{R}$ is the result of a nontrivial interplay between carrier-phonon interlevel scattering and system-reservoir coupling. To better understand this nonequilibrium behavior, we have performed a few simulated experiments based on the electrically-driven quantum-dot model presented so far, varying the ratio $\eta=W^r/W^s$ between carrier-reservoir and phonon-scattering coupling constants. Figure 4 shows (a) the excited- and ground-state carrier populations f_b and f_a and (b) their ratio $\mathcal{R}$ as a function of the coupling-constant ratio η, for an interlevel energy splitting $\Delta\epsilon=25$ meV and for a reservoir-induced population ratio $\mathcal{R}_0=3$ at room temperature. As we can see, for $\eta=0$ (closed-system limit) the thermal-equilibrium value $\mathcal{R}^{\rm eq}=1/e$ is recovered. For increasing values of η we see a progressive increase of the population ratio, which becomes greater than one (population-inversion regime). For $\eta=25$ the resulting population ratio is very close to the scattering-free value $\mathcal{R}_0=3$, which tells us that in such regime the effect of interlevel phonon scattering is negligible.

III. GENERALIZATION TO THE QUANTUM-MECHANICAL CASE

Aim of the present section is to extend the theoretical framework previously introduced to the quantum-mechanical case. To this end, the basic ingredient to be introduced is the so-called single-particle density matrix[5]

$$\rho_{\alpha\beta} = \langle \hat{c}^\dagger_\beta \hat{c}_\alpha \rangle, \tag{14}$$

where $\hat{c}^\dagger_\alpha$ ($\hat{c}_\alpha$) denote creation (destruction) operators for a carrier in state α. This is defined as the average value of two creation and destruction operators: Its diagonal elements correspond to the usual distribution function f_α of the semiclassical Boltzmann theory previously considered, while the off-

diagonal terms ($\alpha \neq \beta$) describe the degree of quantum-mechanical phase coherence between states α and β. Within the usual mean-field and Markov approximations, the time evolution of the single-particle density matrix ρ is dictated by the so-called semiconductor Bloch equations[5–7]

$$\frac{d}{dt}\rho_{\alpha\beta} = \sum_{\alpha'\beta'} L_{\alpha\beta,\alpha'\beta'}\rho_{\alpha'\beta'}, \tag{15}$$

where the effective Liouville operator

$$L_{\alpha\beta,\alpha'\beta'} = \frac{1}{i\hbar}(\epsilon_\alpha - \epsilon_\beta)\delta_{\alpha\beta,\alpha'\beta'} + \Gamma^s_{\alpha\beta,\alpha'\beta'} \tag{16}$$

is the sum of two terms: coherent (i.e., scattering/decoherence-free) single-particle evolution plus energy-relaxation/dephasing dynamics. The latter is described in terms of the scattering tensor Γ^s, whose explicit form, given in Ref. 5, involves the microscopic in- and out-scattering superoperators for the various interaction mechanisms considered, i.e.,

$$\Gamma^s_{\alpha\beta,\alpha'\beta'} = \Gamma^{\text{in}}_{\alpha\beta,\alpha'\beta'} - \Gamma^{\text{out}}_{\alpha\beta,\alpha'\beta'}. \tag{17}$$

Equation (15) is therefore the desired quantum-mechanical generalization of the Boltzmann transport equation in (2). Indeed, by neglecting all nondiagonal terms of the single-particle density matrix ($\rho_{\alpha\beta} = f_\alpha \delta_{\alpha\beta}$), the latter is easily recovered: The "semiclassical elements," $\alpha\alpha' = \beta\beta'$, of the in- and out-scattering matrices in Eq. (17) correspond to the semiclassical scattering rates $P^s_{\alpha\alpha'}$ in Eq. (2). In addition to these so-called semiclassical terms—often referred to as T_1 terms—we have also the so-called T_2 contributions; the latter correspond to the diagonal part of the scattering superoperator Γ^s ($\alpha\beta = \alpha'\beta'$) and describe dephasing processes induced by the various interaction mechanisms considered. The remaining terms in Γ^s describe a nontrivial coupling between diagonal and nondiagonal density-matrix elements. In the presence of T_1 and T_2 terms only—the so-called T_1T_2 model—Eq. (15) has a diagonal, i.e., semiclassical, steady-state solution: $\rho^{\text{s.s.}}_{\alpha\beta} = f^{\text{s.s.}}_\alpha \delta_{\alpha\beta}$. In contrast, as recently pointed out in Ref. 3, the presence of these nontrivial coupling terms between diagonal and nondiagonal density-matrix elements maintains, also in steady-state conditions, a well defined quantum-mechanical phase coherence among different single particle states, which results in a nondiagonal density matrix.

The formulation in terms of the effective Liouville superoperator in (16) recalled so far is typical of a so-called closed system, i.e., a system defined over the whole coordinate space. This is confirmed by the trace-preserving character of the Liouville superoperator L, which corresponds to say that the total number of carriers is preserved.

In order to describe open systems, i.e., systems with open boundaries, a generalization of the conventional SBE in (15) has been recently proposed.[6,7] Within this approach, the spatial boundaries of the systems are incorporated via a generalized Weyl-Wigner treatment of the problem.[7] The resulting equation of motion for the single-particle density matrix is of the form

$$\frac{d}{dt}\rho_{\alpha\beta} = \sum_{\alpha'\beta'} L_{\alpha\beta,\alpha'\beta'}\rho_{\alpha'\beta'} + S_{\alpha\beta} - \sum_{\alpha'\beta'} \Delta L_{\alpha\beta,\alpha'\beta'}\rho_{\alpha'\beta'}, \tag{18}$$

where the presence of spatial boundaries results in a source term S as well as in a renormalization ΔL of the Liouville superoperator in (16). Equation (18) can be schematically written as

$$\frac{d}{dt}\rho_{\alpha\beta} = \left.\frac{d}{dt}\rho_{\alpha\beta}\right|_L + \left.\frac{d}{dt}\rho_{\alpha\beta}\right|_{\text{res}} \tag{19}$$

with

$$\left.\frac{d}{dt}\rho_{\alpha\beta}\right|_{\text{res}} = S_{\alpha\beta} - \sum_{\alpha'\beta'} \Delta L_{\alpha\beta,\alpha'\beta'}\rho_{\alpha'\beta'}. \tag{20}$$

As for the semiclassical case [see Eq. (1)] the global system dynamics is the sum of the dynamics induced by the Liouville superoperator L inside the device active region plus the one induced by the presence of the external reservoirs. While the former is trace preserving, the latter leads, in general, to a variation of the total number of carriers within the spatial region of interest, exactly as for the semiclassical model in Eqs. (1)–(3). Moreover, Eq. (20) exhibits the same injection-minus-loss structure of the relaxation-time-approximation model in (3): the quantum-mechanical source term S corresponds to the semiclassical generation G, while the superoperator ΔL is a nondiagonal generalization of the loss rate γ.

What we propose here is a completely different approach: following the very same strategy introduced in Sec. II, the key idea is again to replace the particle-nonconserving term in (20) with an *ad hoc* scattering superoperator Γ^r describing on a kinetic level the system-reservoir thermalization process. More specifically, similar to Eq. (4), for the quantum-mechanical case we may write

$$\left.\frac{d}{dt}\rho_{\alpha\beta}\right|_{\text{res}} = \sum_{\alpha'\beta'} \Gamma^r_{\alpha\beta,\alpha'\beta'}\rho_{\alpha'\beta'}. \tag{21}$$

Let us now discuss the explicit form of this new scattering superoperator Γ^r. As a first requirement, we shall ask that in the semiclassical limit ($\rho_{\alpha\beta} = f_\alpha \delta_{\alpha\beta}$) Eq. (21) will reduce to Eq. (4). This requires that

$$\Gamma^r_{\alpha\alpha,\alpha'\alpha'} = P^r_{\alpha\alpha'} - \delta_{\alpha\alpha'}\sum_{\alpha''} P^r_{\alpha''\alpha'}. \tag{22}$$

In addition to these semiclassical or T_1 terms, the scattering superoperator Γ^r should also contain dephasing or T_2 contributions. The latter describe, in general, decoherence effects induced by the external reservoir on the carrier subsystem, and will produce a damping of the nondiagonal density-matrix elements; for a given nondiagonal term $\rho_{\alpha\neq\beta}$, the corresponding dephasing rate is given by the average of the total out-scattering rates for states α and β, i.e.,

$$\Gamma^r_{\alpha\beta,\alpha\beta} = -\frac{1}{2}\left(\sum_{\alpha'} P^r_{\alpha'\alpha} + \sum_{\beta'} P^r_{\beta'\beta}\right). \tag{23}$$

As anticipated, in addition to T_1 and T_2 terms, a generic scattering superoperator may also contain additional contributions describing nontrivial couplings between diagonal and nondiagonal density-matrix elements. Such extra terms may lead to a nondiagonal steady-state solution. However, since in the absence of scattering mechanisms inside the simulated region we require a quasithermal, i.e., diagonal, steady-state solution, these extra terms in the scattering superoperator Γ^r are set equal to zero. Combining Eqs. (22) and (23), we finally obtain

$$\Gamma^r_{\alpha\beta,\alpha'\beta'} = \delta_{\alpha\alpha',\beta\beta'}\left(P^r_{\alpha\alpha'} - \delta_{\alpha\alpha'}\sum_{\alpha''} P^r_{\alpha''\alpha'}\right) - \frac{1}{2}\delta_{\alpha\beta,\alpha'\beta'}\left(\sum_{\alpha'} P^r_{\alpha'\alpha} + \sum_{\beta'} P^r_{\beta'\beta}\right). \tag{24}$$

We stress that the only ingredients entering the proposed effective scattering superoperator are the device-reservoir effective scattering rates in (6).

By combining Eqs. (15) and (21), in steady-state conditions, the proposed quantum-transport equation in (19) is given by

$$\frac{d}{dt}\rho_{\alpha\beta} = \sum_{\alpha'\beta'} \mathcal{L}_{\alpha\beta,\alpha'\beta'}\rho_{\alpha'\beta'} = 0 \tag{25}$$

with

$$\mathcal{L}_{\alpha\beta,\alpha'\beta'} = L_{\alpha\beta,\alpha'\beta'} + \Gamma^r_{\alpha\beta,\alpha'\beta'}. \tag{26}$$

By denoting with $i=\alpha\beta$ the generic density-matrix element, the above transport equation can be easily translated into the following homogeneous linear problem:

$$\mathcal{L}_{ii'}\rho_{i'} = 0. \tag{27}$$

In order to show a concrete application of the quantum-mechanical generalization presented so far, let us consider again the electrically driven quantum-dot system previously investigated (see inset in Fig. 4). In this case we deal with a two-by-two density matrix of the form

$$\rho = \begin{pmatrix} \rho_{aa} & \rho_{ab} \\ \rho_{ba} & \rho_{bb} \end{pmatrix} = \begin{pmatrix} f_a & p^* \\ p & f_b \end{pmatrix}. \tag{28}$$

Here, the diagonal elements ρ_{aa} and ρ_{bb} coincide with the semiclassical ground- and excited-state level populations f_a and f_b previously considered [see Eq. (11)], while the nondiagonal element $p=\rho_{ba}$ (together with its complex conjugate $p^*=\rho_{ab}$) describes the degree of quantum-mechanical phase coherence between states a and b. Let us introduce the following (arbitrary) $i=\{\alpha,\beta\}$ mapping: $1=\{a,a\}$, $2=\{b,b\}$, $3=\{b,a\}$, $4=\{a,b\}$. Within such representation, the two-by-two density matrix in (28) is mapped into a four-dimensional vector, and the Liouville superoperator $\mathcal{L}$ in (26) will correspond to a four-by-four matrix.

More specifically, within the four-dimensional mapping given before the transport Eq. (25) in steady-state conditions reduces to the following homogeneous linear problem

$$\begin{pmatrix} \mathcal{L}_{aa,aa} & \mathcal{L}_{aa,bb} & \mathcal{L}_{aa,ba} & \mathcal{L}_{aa,ab} \\ \mathcal{L}_{bb,aa} & \mathcal{L}_{bb,bb} & \mathcal{L}_{bb,ba} & \mathcal{L}_{bb,ab} \\ \mathcal{L}_{ba,aa} & \mathcal{L}_{ba,bb} & \mathcal{L}_{ba,ba} & \mathcal{L}_{ba,ab} \\ \mathcal{L}_{ab,aa} & \mathcal{L}_{ab,bb} & \mathcal{L}_{ab,ba} & \mathcal{L}_{ab,ab} \end{pmatrix} \begin{pmatrix} f_a \\ f_b \\ p \\ p^* \end{pmatrix} = 0, \tag{29}$$

where $\mathcal{L}$ is the sum of a closed-system operator L and a corresponding system-reservoir scattering superoperator Γ^r [see Eq. (26)].

The explicit form of L for our simplified two-level model is given by

$$\begin{pmatrix} L_{aa,aa} & L_{aa,bb} & L_{aa,ba} & L_{aa,ab} \\ L_{bb,aa} & L_{bb,bb} & L_{bb,ba} & L_{bb,ab} \\ L_{ba,aa} & L_{ba,bb} & L_{ba,ba} & L_{ba,ab} \\ L_{ab,aa} & L_{ab,bb} & L_{ab,ba} & L_{ab,ab} \end{pmatrix} = \frac{1}{i\hbar}\begin{pmatrix} 0 & 0 & 0 & 0 \\ 0 & 0 & 0 & 0 \\ 0 & 0 & \Delta\epsilon & 0 \\ 0 & 0 & 0 & -\Delta\epsilon \end{pmatrix} + \begin{pmatrix} \Gamma^s_{aa,aa} & \Gamma^s_{aa,bb} & \Gamma^s_{aa,ba} & \Gamma^s_{aa,ab} \\ \Gamma^s_{bb,aa} & \Gamma^s_{bb,bb} & \Gamma^s_{bb,ba} & \Gamma^s_{bb,ab} \\ \Gamma^s_{ba,aa} & \Gamma^s_{ba,bb} & \Gamma^s_{ba,ba} & \Gamma^s_{ba,ab} \\ \Gamma^s_{ab,aa} & \Gamma^s_{ab,bb} & \Gamma^s_{ab,ba} & \Gamma^s_{ab,ab} \end{pmatrix} \tag{30}$$

with

$$\begin{pmatrix} \Gamma^s_{aa,aa} & \Gamma^s_{aa,bb} & \Gamma^s_{aa,ba} & \Gamma^s_{aa,ab} \\ \Gamma^s_{bb,aa} & \Gamma^s_{bb,bb} & \Gamma^s_{bb,ba} & \Gamma^s_{bb,ab} \\ \Gamma^s_{ba,aa} & \Gamma^s_{ba,bb} & \Gamma^s_{ba,ba} & \Gamma^s_{ba,ab} \\ \Gamma^s_{ab,aa} & \Gamma^s_{ab,bb} & \Gamma^s_{ab,ba} & \Gamma^s_{ab,ab} \end{pmatrix} = W^s \begin{pmatrix} -N & N+1 & 0 & 0 \\ N & -(N+1) & 0 & 0 \\ \frac{i}{2}\lambda N & -\frac{i}{2}\lambda(N+1) & -\frac{1}{2}(2N+1) & \frac{1}{2}(2N+1) \\ -\frac{i}{2}\lambda N & \frac{i}{2}\lambda(N+1) & \frac{1}{2}(2N+1) & -\frac{1}{2}(2N+1) \end{pmatrix}, \tag{31}$$

where the dimensionless parameter $i\lambda$ depends on the explicit form of the carrier wave functions associated with our two-level system.[18] As already stressed, by neglecting $f \rightarrow p$ terms (which corresponds to set $\lambda = 0$), populations and polarizations are totally decoupled. In contrast, in the presence of these T_3 terms our steady-state solution exhibit a residual single-particle coherence, i.e., a polarization p different from zero.

Let us now come to the system-reservoir effective scattering superoperator in (24). Its explicit form for our two-level system is

$$\begin{pmatrix} \Gamma^r_{aa,aa} & \Gamma^r_{aa,bb} & \Gamma^r_{aa,ba} & \Gamma^r_{aa,ab} \\ \Gamma^r_{bb,aa} & \Gamma^r_{bb,bb} & \Gamma^r_{bb,ba} & \Gamma^r_{bb,ab} \\ \Gamma^r_{ba,aa} & \Gamma^r_{ba,bb} & \Gamma^r_{ba,ba} & \Gamma^r_{ba,ab} \\ \Gamma^r_{ab,aa} & \Gamma^r_{ab,bb} & \Gamma^r_{ab,ba} & \Gamma^r_{ab,ab} \end{pmatrix} = \frac{W^r}{\mathcal{R}_0 + 1} \begin{pmatrix} -\mathcal{R}_0 & 1 & 0 & 0 \\ \mathcal{R}_0 & -1 & 0 & 0 \\ 0 & 0 & -\frac{1}{2}(\mathcal{R}_0 + 1) & \frac{1}{2}(\mathcal{R}_0 + 1) \\ 0 & 0 & \frac{1}{2}(\mathcal{R}_0 + 1) & -\frac{1}{2}(\mathcal{R}_0 + 1) \end{pmatrix}. \tag{32}$$

Let us now present a few simulated experiments for the electrically driven quantum-dot system previously considered (see inset in Fig. 4) based on the quantum-mechanical generalization proposed in this section. To this end, let us start by investigating the closed-system limit, i.e., no system-reservoir coupling ($W^r = 0$).

Figure 5 shows the modulus of the interlevel polarization p as a function of the dimensionless coupling parameter $\Lambda = \hbar W^s / \Delta\epsilon$. In this numerical example we have chosen $\Delta\epsilon = 25$ meV, $T = 300$ K, and $\lambda = 0.4$. As we can see, $|p|$ comes out to be proportional to the coupling parameter Λ, as can be readily verified by a closer inspection of our four-by-four superoperator L in (30). It follows that for any finite value of the coupling parameter Λ, we deal with a nondiagonal steady-state solution ρ [see Eq. (28)]. More specifically, its diagonal elements f_a and f_b are Λ-independent and correspond to the semiclassical equilibrium distribution: $f_b / f_a = N/N+1$; the nondiagonal elements p and p^* will increase linearly with the coupling parameter Λ. It is possible to show that for small/moderate values of Λ our two-by-two density matrix is positive-definite, which suggests the introduction of a dressed-state basis in which the latter is diagonal. The new populations $\overline{f_a}$ and $\overline{f_b}$ (dashed curves in Fig. 5) can be regarded as the average occupation of such dressed states. As we can see, for $\Lambda = 0$ they coincide with the noninteracting thermal ones; for increasing values of the carrier-phonon coupling the population ratio $\overline{f_b} / \overline{f_a}$ decreases. Such a behavior can be physically described in terms of a phonon-induced renormalization of the interlevel energy splitting $\Delta\epsilon$. Indeed, such renormalized transition energy can also be obtained from the imaginary parts of the non-zero eigenvalues of the effective Liouville operator in (30). We stress that such bidimensional dressed basis, as well as the corresponding energy shift, can be regarded as the simplest example of polaronic phase-coherence and state renormalization.

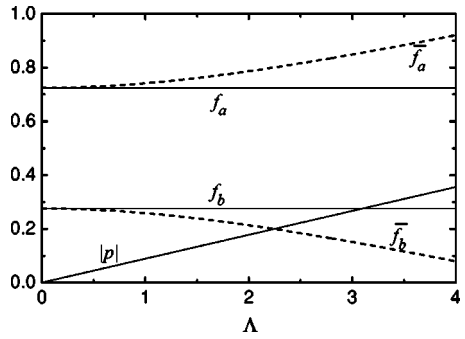

FIG. 5. Phonon-induced single-particle phase coherence for an isolated quantum-dot system: modulus of the interlevel polarization $|p|$ (solid curve) and dressed-state populations $\overline{f_b}$ and $\overline{f_a}$ (dashed curves) as a function of the coupling-constant ratio Λ, for an interlevel energy splitting $\Delta\epsilon = 25$ meV at room temperature (see text).

Let us now discuss the quantum-mechanical generalization of the open-system scenario described in Fig. 4. Figure 6 shows the ground- and excited-level populations (dashed curves) as well as the modulus of the interlevel polarization (solid curve) as a function of the coupling-parameter ratio $\eta = W^r / W^s$ at room temperature for a fixed value of the scattering coupling constant: $\hbar W^s = 25$ meV. As we can see, exactly as in the semiclassical case (see Fig. 4), for increasing values of η we enter a pronounced nonequilibrium regime, leading eventually to a reservoir-induced population inversion.

More important, the present quantum-mechanical treatment allows us to study the effect of the external reservoirs on the phonon-induced single-particle phase coherence (see Fig. 5). Indeed, for increasing values of the system-reservoir coupling W^r we experience a progressive decrease of the interlevel polarization p, which is a clear fingerprint of a decoherence/dephasing effect induced by the external reservoir.

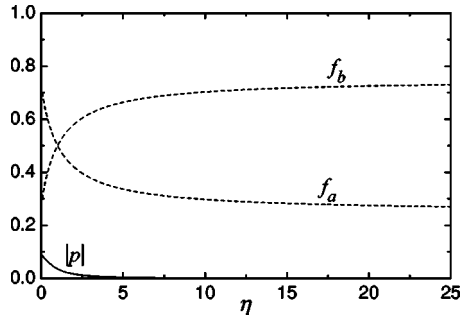

FIG. 6. Quantum-mechanical simulation of the electrically driven nonequilibrium carrier dynamics for the quantum-dot system of Fig. 4: excited- and ground-state populations f_b and f_a (dashed curves) and modulus of the interlevel polarization $|p|$ as a function of the coupling-constant ratio η, for an interlevel energy splitting $\Delta\epsilon = 25$ meV and for a reservoir-induced population ratio $\mathcal{R}_0 = 3$ at room temperature (see text).

IV. SUMMARY AND CONCLUSIONS

In summary, we have proposed an alternative simulation strategy for the study of nonequilibrium carrier dynamics in quantum devices with open boundaries: the key idea is to replace the usual modeling of open quantum systems based on phenomenological injection/loss rates with a kinetic description of the system-reservoir thermalization process. In particular, within this simulation scheme the partial carrier thermalization induced by the device spatial boundaries is treated via a conventional Boltzmann-theory approach in terms of an effective collision operator between the highly nonthermal device electrons and the thermal carrier distribution of the reservoir. In this approach the total number of simulated electrons is preserved (closed scheme); this is a distinguished advantage of the proposed strategy, compared to hybrid—direct numerical-integration plus MC-sampling—schemes, where the total number of particles is not preserved (open scheme).

Finally, we have extended the proposed particle-conserving kinetic approach to the quantum-transport regime. More specifically, as for the semiclassical case, we have introduced a Liouville superoperator able to properly describe carrier thermalization/dephasing induced by the device spatial boundaries.

Within the semiclassical scenario, by replacing the conventional injection/loss model with a Boltzmann-like effective scattering operator, we are able to move from an open to a closed scheme, prerequisite for the application of the well-established ensemble MC method. Following this spirit, we have presented a few simulated experiments of hot-carrier dynamics in semiconductor-based quantum devices, namely double-barrier structures and electrically driven quantum-dot systems. These simulated experiments have fully confirmed its validity as well as its power and flexibility.

Finally, the proposed quantum-mechanical generalization of the theory has been successfully applied to the study of environment-induced dephasing in electrically-driven quantum-dot systems. We stress that the proposed trace-preserving Liouville superoperator—contrary to other formulations of the problem[7]—ensures the positive-definite character of the steady-state density matrix,[19] thus allowing for the usual probabilistic interpretation of our simulated experiments.

*Email address: proietti@athena.polito.it
†Email address: emanuele.ciancio@polito.it
‡Email address: rita.iotti@infm.polito.it
§Email address: fausto.rossi@polito.it

[1] See, e.g., C. Jacoboni and P. Lugli, *The Monte Carlo Method for Semiconductor Device Simulations* (Springer, Wien, 1989).
[2] See, e.g., *Theory of Transport Properties of Semiconductor Nanostructures*, edited by E. Schöll (Chapman & Hall, London, 1998).
[3] See, e.g., R.C. Iotti and F. Rossi, Phys. Rev. Lett. **87**, 146603 (2001).
[4] See, e.g., W. Frensley, Rev. Mod. Phys. **62**, 745 (1990), and references therein.
[5] See, e.g., F. Rossi and T. Kuhn, Rev. Mod. Phys. **74**, 895 (2002), and references therein.
[6] F. Rossi, A. Di Carlo, and P. Lugli, Phys. Rev. Lett. **80**, 3348 (1998).
[7] R. Proietti Zaccaria and F. Rossi, Phys. Rev. B **67**, 113311 (2003).
[8] See, e.g., *Special Issue on Computational Electronics*, VLSI Des. **13** (2001).
[9] See, e.g., *Special Issue Featuring Papers from the International Conference on Nonequilibrium Carrier Dynamics in Semiconductors*, Semicond. Sci. Technol. **19** (2004).
[10] M.V. Fischetti, Phys. Rev. B **59**, 4901 (1999), and references therein.
[11] The proposed theoretical approach does not account for Schrödinger-Poisson corrections. Its reformulation to include such self-consistency effects, although straightforward, is outside the scope of the present paper.
[12] The decomposition in Eq. (1) is not obvious; a derivation can be found in R.C. Iotti and F. Rossi, phys. stat. sol. (b) **238**, 462 (2003).
[13] Within a scattering-state picture, the quantum number associated to the generic state α is the longitudinal carrier wave vector far from the device active region; the ballistic transit time is then the ratio between the length of the active region and the longitudinal carrier velocity.
[14] See, e.g., R.C. Iotti and F. Rossi, Appl. Phys. Lett. **76**, 2265 (2000).
[15] For the case of a nonequilibrium carrier distribution f^0_α, the detailed-balance principle should be replaced by a total-balance one. However, by inserting Eq. (6) into the effective collision operator in (4) it is easy to verify that its steady-state solution is $f_\alpha = f^0_\alpha$.
[16] Since in the simulated experiments discussed below we shall focus on low density conditions, carrier-carrier scattering has not been considered.
[17] To compare the transient response of the two models it is useful to assume identical initial conditions. To this end we have also simulated the open system starting from the same initial distribution considered in (b). The resulting current density as a function of time (not reported here) coincides within a few percents with the dashed curve in (c).
[18] In our simplified model we assume real and symmetric wavefunctions which guarantee that λ is a real number.
[19] This is true in the weak coupling regime. In case of strong coupling, however, the whole perturbative approach on which the derivation is based fails.